

Computer analysis of oxygen adsorption at SnO₂ thin films

WERONIKA IZYDORCZYK^{1*}, BOGUSŁAWA ADAMOWICZ²

¹Institute of Electronics, Silesian University of Technology, Akademicka 16, 44-100 Gliwice, Poland

²Department of Applied Physics, Institute of Physics, Silesian University of Technology, Bolesława Krzywoustego 2, 44-100 Gliwice, Poland

*Corresponding author: Weronika.Izydorzcyk@polsl.pl

An influence of oxidation of SnO₂ thin films on depletion layer electronic parameters and film conductance has been studied by means of computer simulations. The surface potential value and in-depth potential profiles in the depletion region have been obtained by solving the Poisson–Boltzmann equation in the case of grains with slab geometry and different doping. The SnO₂ grain thickness was in the range from 20 to 500 nm. The surface coverage by oxygen ions (O₂⁻, O⁻) as well as film conductance per square and its sensitivity versus temperature (from 300 to 900 K) have been rigorously calculated. The effect of donor (oxygen vacancies) mobility and degree of donor ionisation has been taken into account.

Keywords: SnO₂ thin films, nanolayers, oxygen adsorption, depletion layer, modeling of sensor structures.

1. Introduction

The surface space charge region in metal-oxide semiconductors, *i.e.* SnO₂, which decides about the operation of resistive gas sensors, is formed due to both adsorption of gas molecules and ionization of surface states related to the oxygen vacancies at the surface [1, 2]. The surface-related phenomena become particularly important for nanomaterials which exhibit a much higher surface-to-volume ratio compared to SnO₂ thick films composed of micro-grains. Therefore, the understanding and control of the surface and near-surface electronic properties and their relationship with material ones are key factors for technology optimization, and thus for an improvement of the sensitivity and selectivity of SnO₂-based sensor devices [3]. Furthermore, the modeling of sensor structures based on nanolayers needs to consider the size and shape of grains, which decide about the layer conductance. It is well known that

in the case of metal-oxide semiconductors oxygen in various forms plays a crucial role in gas sensing due to its reactivity. In spite of many experimental and theoretical studies [4–14], the role of oxygen adsorption in surface and bulk phenomena (surface coverage by oxygen, band bending, mobile donor distribution) in nanostructured SnO₂ films and its influence on film conductance is not clear. The oxygen adsorbs on the surface in such forms like O₂, O₂⁻, O⁻, and O²⁻. The investigations on SnO₂ surface using electron paramagnetic resonance (EPR) [4] indicates that below 200 °C the molecular species O₂⁻ are present on the surface SnO₂, while atomic species O⁻ become dominant above 150–200 °C at low oxygen pressure. According to the literature reports, the oxygen ion O⁻ plays a special role in the catalytic surface processes and induces the electrical changes in SnO₂ layers in the temperature range from about 500 to 800 K. The surface coverage by oxygen (surface concentration of adsorbed species per surface concentration of adsorption sites) is independent of temperature and oxygen pressure for moderate values of pressure [5]. However, the ratio of O₂⁻ to O⁻ concentration increases with the oxygen pressure. The reversible changes in the conductance of SnO₂ films with oxygen partial pressure were observed at temperatures of sensor operation above 500 K [6]. The conductance changes followed a power law $G \sim [p_{O_2}]^\alpha$, where values of α are usually between -0.25 and -0.5 [6–7] or $\alpha = -1/6$ at temperatures above 1000 K [8]. The band bending induced by chemisorbed oxygen was observed by MIZSEI *et al.* [9] and SEMANCIK *et al.* [10]. Furthermore, the X-ray photoelectron spectroscopy (XPS) studies of nanocrystalline SnO₂ films showed an upward band bending of 0.2 eV after the exposure to O₂ [11]. The adsorption of O₂ on a stoichiometric surface as well as at oxygen vacancies was investigated theoretically [12, 13]. The effect of grain geometry on the height of the surface energy barrier in the case of constant surface donor concentration was investigated by RANTALA *et al.* [14]. The surface energy barriers (up to 0.7 eV) were calculated for different sizes of full-depleted grains in the case of mobile singly ionised and doubly ionised donors for slab, cylindrical and spherical grain geometries. These studies proved that tin dioxide thin films may be fully depleted from electrons in the atmospheric air. The maximum grain radii, above which the full depletion is no longer possible, were about 0.25 and 1 μm at temperature $T = 573$ K in the case of mobile singly and doubly ionised donors, respectively. Thus, modelling of sensor structures based on nanostructured SnO₂ layers requires the consideration of grain size and shape.

The aim of this work is a rigorous theoretical analysis of the influence of surface oxidation on the conductance of SnO₂ nano-films, which was not reported in the literature yet. From the one-dimensional analytical solution of the Poisson–Boltzmann equation in the case of grains with slab geometry (1D), the in-depth potential profiles were obtained. Full-depleted layer due to the adsorption of oxygen molecules at SnO₂ surface was assumed following [14]. The SnO₂ grain thickness was in the range from 20 to 500 nm. On this basis, the dependence of the surface energy barriers on temperature (from 300 to 900 K) and different doping was determined. These solutions were used as input data to computer simulations based on the rate equations proposed

by RANTALA *et al.* [1] for the electron transfer between the oxygen surface species and the bulk conduction band in order to calculate the total coverage by oxygen species and coverages by various oxygen ions. Subsequently, the in-depth profiles of carrier concentrations and temperature dependencies of the conductance per square under various partial oxygen pressures were obtained. Furthermore, the SnO₂ film sensitivity with respect to temperature and oxygen partial pressure versus temperature and film thickness was calculated. In our approach to the oxygen adsorption mechanism at SnO₂ surface, the effect of donor (oxygen vacancies) mobility and the degree of donor ionisation was taken into account.

2. Computer procedure

The in-depth potential profiles in the depletion region induced by gas adsorption and surface energy barrier heights were computed for one-dimensional SnO₂ grains with slab geometry (*i.e.*, grain thickness $2 \times L$ is much lower than other dimensions) and n-type doping (donor concentration N_d). The electric potential $\phi(r)$ was obtained by solving the Poisson–Boltzmann equation:

$$\frac{d^2 \phi(r)}{dr^2} = -\frac{emN_{d_0}}{\varepsilon\varepsilon_0} \exp[-m\beta\phi(r)] + \frac{en_0}{\varepsilon\varepsilon_0} \exp[\beta\phi(r)] \quad (1)$$

where r is the distance from the grain centre, e is the elementary charge, $\beta = e/k_bT$, $m = 1$ for single donors and $m = 2$ for double donors, $\varepsilon\varepsilon_0$ is the semiconductor permittivity; N_{d_0} and n_0 are the donor and electron concentrations in the centre ($r = 0$) of the slab, determined by the following formulas, respectively:

$$N_{d_0} = N_{d_s} \exp(m\beta\phi_s) \quad (2)$$

$$n_0 = n_s \exp(-\beta\phi_s) \quad (3)$$

where N_{d_s} and n_s are the donor and electron concentrations at the surface, ϕ_s is the surface potential.

The first and second boundary conditions are $\phi(r=0) = 0$ and $d\phi/dr = 0$ in the grain centre $r = 0$ [14]. The first term in Eq. (1) represents the contribution of the mobile donors at the temperature T , whereas the second term including the charge distribution of electrons was neglected due to the total depletion assumption [14].

The analytical solution of Eq. (1) gives for the electric potential the following expression:

$$\phi(r) = -\frac{1}{m\beta} \ln \left[1 + \tan^2 \left(\frac{r}{\lambda} \right) \right] \quad (4)$$

and for the distribution of bulk donor concentration:

$$N_d(r) = N_{d_0} \left[1 + \tan^2 \left(\frac{r}{\lambda} \right) \right] \quad (5)$$

where:

$$\lambda^{-1} = \sqrt{\frac{em^2 \beta N_{d_0}}{2 \varepsilon \varepsilon_0}} \quad (6)$$

Assuming that N_d is uniform in the bulk in no oxygen-containing atmosphere, we can write:

$$\int_0^L N_d(r) dr = N_d L \quad (7)$$

It should be noted that in our approach the surface donor concentration N_{d_s} was not a constant value, contrary to the assumption in [14].

The surface potential ϕ_s for different temperatures, layer thickness and doping was obtained by solving the system of equations (2) and (4)–(7). The ϕ_s values were then applied as input data in the calculations of the surface total coverage with oxygen ions, coverage with various oxygen ions, and thus carrier concentration in-depth profile in the depletion layer. These simulations were based on the solving of rate equations following [1]. In our approach based on the adsorption-desorption model proposed by RANTALA *et al.* [1] all possible surface reactions and phenomena, *i.e.*, multi-step oxygen adsorption, dissociation, recombination, and desorption, were taken into account. As a result of adsorption, the negative charge trapped at oxygen species causes an upward band bending and thus a reduced conductivity compared to the flat band condition. The parameters related to the gas adsorption modelling and necessary for simulation of the surface coverage by oxygen ions O_2^- and O^- , including the capture cross-section, sticking coefficient, activation energies, and vibration frequency of O_2 were taken from [1, 15].

The sample conductance was determined from the classical formula [5, 16] using the obtained carrier concentration in-depth profiles. Because of the high doping of n-type SnO_2 , the hole concentration was neglected. Furthermore, the temperature sensitivity S_T and gas pressure sensitivity α were calculated from standard formulas. The calculations were carried out for n- SnO_2 layers with different thickness, from 20 to 500 nm, and doping level (single or double mobile bulk oxygen vacancies [17]) from $N_d = 2.5 \times 10^{18} \text{ cm}^{-3}$ to $N_d = 2.5 \times 10^{19} \text{ cm}^{-3}$ and within the temperature range from 300 to 900 K. We assumed the following carrier parameters: electron mobility

$\mu_e = 150 \text{ cm}^2\text{V}^{-1}\text{s}^{-1}$ at 300 K, and effective mass of electron equal to $0.3 m_e$, where m_e is the electron rest mass. The temperature variations in the carrier mobility were taken from [18, 19].

3. Results and discussion

The calculated in-depth potential profiles of the full depletion layer in the n-SnO₂ slab with the thickness $2 \times L = 20 \text{ nm}$ (at 600 K) upon oxygen adsorption for different initial (no-gas condition) mobile bulk donor concentration N_d are presented in Fig. 1a. The corresponding values of the surface energy barrier versus temperature (from 300 to 900 K) and N_d are shown in Fig. 1. From Fig. 1a it results that the surface potential changes markedly (from about -0.12 to -0.4 V) while the doping increases by one order of magnitude (from 2.5×10^{18} to $2.5 \times 10^{19} \text{ cm}^{-3}$). On the other hand, the similar large change in the surface energy barrier height was observed upon a temperature increase from 300 to 900 K for a slab with high donor concentration $N_d = 10^{19} \text{ cm}^{-3}$ (Fig. 1b). Furthermore, the surface barriers are shown to increase with increasing donor concentration N_d at all temperatures and for different layer thickness. It should be also noted that the calculated values of the surface barriers (see Fig. 1a) for a constant value of donor concentration near the surface $N_{ds} = 10^{20} \text{ cm}^{-3}$, are consistent with those obtained by RANTALA *et al.* [14].

The full depletion layer was induced by the electrons captured at adsorbed oxygen species (O^- and O_2^-). Their total concentration at the surface depends on complex processes of adsorption, dissociation, recombination, and desorption. The calculated total coverage by oxygen species as well coverages by oxygen ions O^- and O_2^- versus temperature in dry synthetic air (20% oxygen content), for singly ionised donors ($N_d = 3 \times 10^{18} \text{ cm}^{-3}$, $L = 250 \text{ nm}$) and for doubly ionised donors ($N_d = 6 \times 10^{18} \text{ cm}^{-3}$,

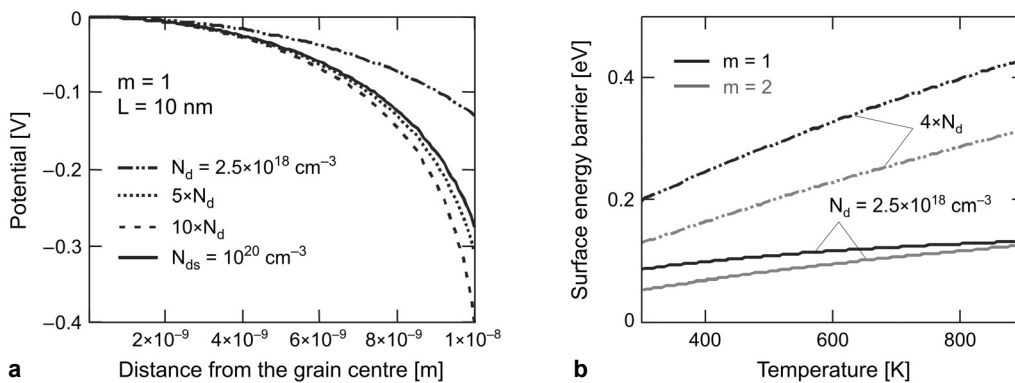


Fig. 1. Calculated in-depth potential profiles in SnO₂ slabs at $T = 600 \text{ K}$ (a) and surface energy barriers vs. temperature (b) for different donor concentrations; $L = 10 \text{ nm}$, $m = 1$ or 2. The solid line in (a) corresponds to the assumption $N_{ds} = \text{const}$ after [14].

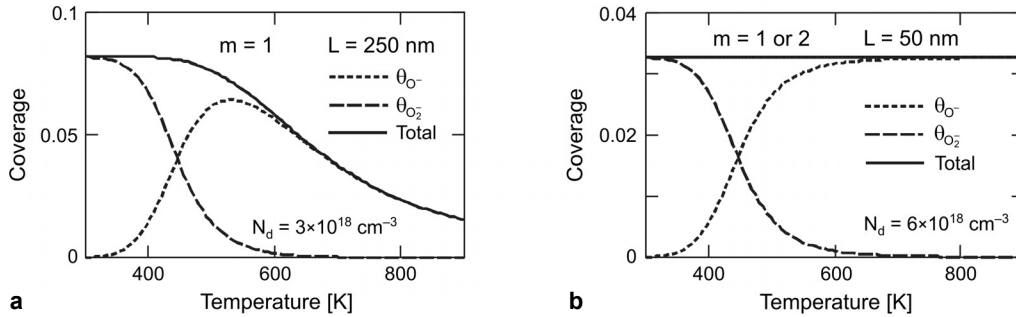


Fig. 2. Calculated SnO₂ surface coverage by the oxygen ions O⁻ and O₂⁻ and total coverage (O⁻ + O₂⁻) vs. temperature in dry synthetic air, for mobile singly ionized donor concentration $N_d = 3 \times 10^{18} \text{ cm}^{-3}$, $L = 250$ nm (a) and for single and doubly ionized donor concentration $N_d = 6 \times 10^{18} \text{ cm}^{-3}$, $L = 50$ nm (b).

$L = 50$ nm) are shown in Fig. 2. The dynamics of changes in the total coverage depends on the grain thickness and in the case of thin slabs is very weak (Fig. 2b). Furthermore, the coverages by the atomic and molecular ionic species are equal at the temperature of about 445 K. It should be noted that this value is comparable to the transition temperature of 423 K obtained from the measurements by CHANG [4] on SnO₂ nanolayers (~ 100 nm) deposited onto an alumina substrate by reactive sputtering from a sintered tin oxide target and by REMBEZA *et al.* [20] on magnetron sputtered nanocrystalline (grain dimension < 20 nm) tin dioxide films (thickness $> 1 \mu\text{m}$) on glass substrates.

The surface space charge region, induced by adsorbed ions, contributes significantly to the conductance of the semiconducting SnO₂ layers. The sample conductance per square was determined from the classical formula [5, 16] using the obtained in-depth carrier profiles. The dependence of the conductance per square on temperature for different partial pressure of oxygen and slab thickness is shown in Fig. 3. From our calculations it results that in the case of thicker SnO₂ layer ($2 \times L = 250$ nm) the maximum conductance per square is shifted towards lower temperatures for a lower partial pressure of oxygen (Fig. 3a). The maximum conductance due to oxygen adsorption was experimentally observed both at the temperature 450 K for nanocrystalline SnO₂ films (grain dimension < 20 nm) [20] and between 550 and 600 K for polycrystalline thin film of thickness lower than 500 nm and an average grain size equal to 15 nm [21]. Large differences in measurements of film conductance depend on differences in the surface stoichiometry, layer smoothness, type of substrate and different techniques of film fabrication [22].

For the slab with thickness 100 nm (Fig. 3b) the values of the conductance per square are three orders of magnitude lower than for a thicker slab (500 nm) (Fig. 3a) due to a higher contribution from the depletion layer. One can also note that for relatively low oxygen concentration a strong change in the conductance of the thinner sample versus temperature is observed (Fig. 3b). The calculated dependences of the sensitivity with respect to oxygen partial pressure α versus

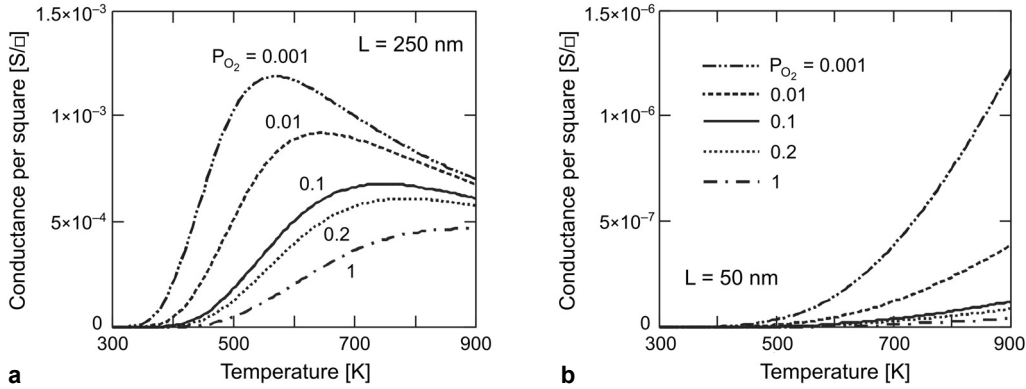


Fig. 3. Calculated conductance per square vs. temperature for different oxygen partial pressure P_{O_2} and $N_d = 3 \times 10^{18} \text{ cm}^{-3}$, $L = 250 \text{ nm}$, $m = 1$ (a) and $N_d = 6 \times 10^{18} \text{ cm}^{-3}$, $L = 50 \text{ nm}$, $m = 2$ (b).

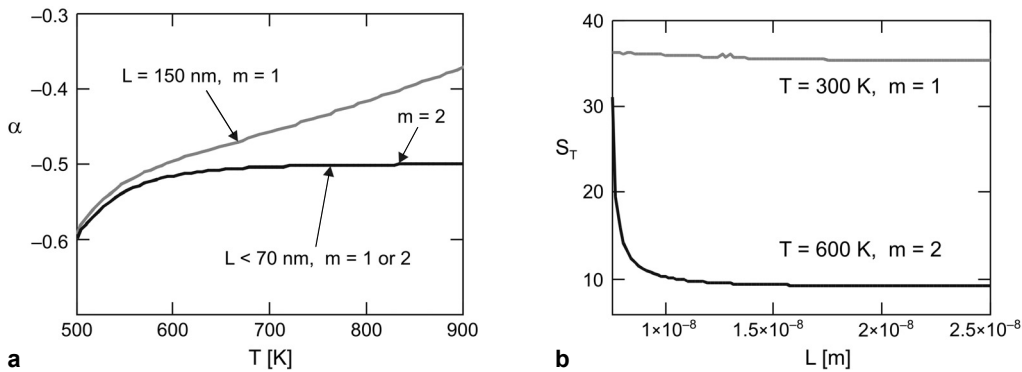


Fig. 4. Calculated sensitivity with respect to oxygen partial pressure in ambient atmosphere α vs. temperature, for $N_d = 3 \times 10^{18} \text{ cm}^{-3}$ (a) and sensitivity with respect to temperature S_T vs. the half of the slab thickness L for $N_d = 1 \times 10^{18} \text{ cm}^{-3}$ (b) for single $m = 1$ and double $m = 2$ mobile donors.

temperature and sensitivity with respect to temperature S_T versus the half of slab thickness L for different ionization degree ($m = 1$ and 2), are summarized in Fig. 4. As it results from Fig. 4a, the parameter α is slightly dependent on the degree of donor ionization for the slab thickness lower than 150 nm. The value of α changes in the range from -0.6 to -0.38 for the layer temperature between 500 and 900 K. This result is consistent with [23] where the calculations performed on the basis of acting mass law give for the $\alpha = -0.5$ constant concentration of oxygen lattice defects (oxygen vacancies). Experimentally, the values of α were about -0.38 for porous SnO₂ thick films [7] and -0.5 for polycrystalline thin films, where the grain size changed between 100 and 500 nm [6]. From Fig. 4b it is evident that the parameter S_T strongly depends on the grain thickness and degree of donor ionization. This value rises three times for a slab thickness decreasing from 30 to 15 nm in the case of mobile doubly ionized donors at 600 K and for $N_d = 10^{18} \text{ cm}^{-3}$.

4. Conclusions

The surface energy barrier and in-depth potential profiles in the depletion layer induced under oxygen adsorption at SnO₂ grains with 1D slab geometry were analysed in details as a function of mobile donor concentration in a wide range of temperature (from 300 to 900 K). Our computer analysis showed that the temperature changes of the surface coverage with ionised oxygen species (O₂⁻ and O⁻) as well as layer conductance are dependent on the slab thickness (in the range from 20 to 500 nm). The calculated SnO₂ slab sensitivity with respect to the oxygen partial pressure α and temperature S_T for different donor ionization degree, revealed the marked variations of S_T versus slab thickness. The obtained α values are consistent with experimental and theoretical data reported in the literature.

The performed theoretical analysis for SnO₂ slabs exposed to oxygen is a good approximation of the electronic properties of SnO₂-based gas sensors with thin epitaxial layers or small grains, where the depletion layer thickness is comparable to grain thickness.

Acknowledgements – This work was sponsored by the Polish Ministry of Science and Higher Education within a research project 1391/T02/2007/32. The authors thank Dr. Nicolae Bârsan and Dr. Dorota Koziej from the Institute of Physical and Theoretical Chemistry, University of Tübingen, Germany for precious discussions. The support from the GOSPEL No EC IST 507610 is acknowledged.

References

- [1] RANTALA T.S., LANTTO V., RANTALA T.T., *Rate equation simulation of the height of Schottky barriers at the surface of oxidic semiconductors*, Sensors and Actuators B: Chemical **13–14**, 1993, pp. 234–7.
- [2] IZYDORCZYK W., ADAMOWICZ B., MICZEK M., WACZYŃSKI K., *Computer analysis of an influence of oxygen vacancies on the electronic properties of the SnO₂ surface and near-surface region*, Physica Status Solidi A **203**(9), 2006, pp. 2241–6.
- [3] SZUBER J., CZEMPIK G., LARCIPRETE R., ADAMOWICZ B., *The comparative XPS and PYS studies of SnO₂ thin films prepared by L-CVD technique and exposed to oxygen and hydrogen*, Sensors and Actuators B: Chemical **70**(1–3), 2000, pp. 177–81.
- [4] CHANG S.C., *Oxygen chemisorption on tin oxide: Correlation between electrical conductivity and EPR measurements*, Journal of Vacuum Science and Technology **17**(1), 1980, pp. 366–9.
- [5] MORRISON S.R., *The Chemical Physics of Surfaces*, Plenum Press, New York 1997.
- [6] KISSINE V.V., SYSOEV V.V., VOROSHILOV S.A., *Conductivity of SnO₂ thin films in the presence of surface adsorbed species*, Sensors and Actuators B: Chemical **79**(2–3), 2001, pp. 163–70.
- [7] LANTTO V., ROMPPAINEN P., LEPPÄVUORI S., *Response studies of some semiconductor gas sensors under different experimental conditions*, Sensors and Actuators **15**(4), 1988, pp. 347–57.
- [8] SCHIERBAUM K.D., WIEMHÖFER H.D., GÖPEL W., *Defect structure and sensing mechanism of SnO₂ gas sensors: comparative electrical and spectroscopic studies*, Solid State Ionics, Diffusion and Reactions **28–30**, 1988, pp. 1631–6.
- [9] MIZSEI J., LANTTO V., *Simultaneous response of work function and resistivity of some SnO₂-based samples to H₂ and H₂S*, Sensors and Actuators B: Chemical **4**(1–2), 1991, pp. 163–8.
- [10] SEMANCIK S., COX D.F., *Fundamental characterization of clean and gas-dosed tin oxide*, Sensors and Actuators **12**(2), 1987, pp. 101–6.

- [11] MAFFEIS T.G.G., OWEN G.T., PENNY M.W., STARKE T.K.H., CLARK S.A., FERKEL H., WILKS S.P., *Nanocrystalline SnO₂ sensor response to O₂ and CH₄ at elevated temperature investigated by XPS*, *Surface Science* **520**(1–2), 2002, pp. 29–34.
- [12] SLATER B., CATLOW C.R.A., WILLIAMS D.E., STONEHAM A.M., *Dissociation of O₂ on the reduced SnO₂ (110) surface*, *Chemical Communications*, Issue 14, 2000, pp. 1235–6.
- [13] OVIEDO J., GILLAN M.J., *First-principles study of the interaction of oxygen with the SnO₂ (110) surface*, *Surface Science* **490**(3), 2001, pp. 221–36.
- [14] RANTALA T.S., LANTTO V., *Some effects of mobile donors on electron trapping at semiconductor surfaces*, *Surface Science* **352–354**, 1996, pp. 765–70.
- [15] MORRISON S.R., *Mechanism of semiconductor gas sensor operation*, *Sensors and Actuators* **11**(3), 1987, pp. 283–7.
- [16] BARSAN N., WEIMAR U., *Conduction model of metal oxide gas sensor*, *Journal of Electroceramics* **7**(3), 2001, pp. 143–67.
- [17] MURAKAMI N., TANAKA K., SASAKI K., IKOHURA K., *Proceedings of the International Meeting on Chemical Sensors*, Fukuoka, Japan, September 19–22, 1983, p. 187.
- [18] SUMMIT H.R., BORRELLI N.F., *Temperature dependence of the ultraviolet absorption edges in SnO₂*, *Journal of Applied Physics* **37**(5), 1966, pp. 2200–1.
- [19] FONSTAD C.G., REDIKER R.H., *Electrical properties of high-quality stannic oxide crystals*, *Journal of Applied Physics* **42**(7), 1971, pp. 2911–8.
- [20] REMBEZA S.I., REMBEZA E.S., SVISTOVA T.V., BORSIAKOVA O.I., *Electrical resistivity and gas response mechanisms of nanocrystalline SnO₂ films in a wide temperature range*, *Physica Status Solidi A* **179**(1), 2000, pp. 147–52.
- [21] SANJINES R., LÉVY F., DEMARNE V., GRISEL A., *Some aspects of the interaction of oxygen with polycrystalline SnO_x thin films*, *Sensors and Actuators B: Chemical* **B1**(1–6), 1990, pp. 176–82.
- [22] VETRONE J., CHUNG Y.W., CAVICCHI R., SEMANCIK S., *Role of initial conductance and gas pressure on the conductance response of single-crystal SnO₂ thin films to H₂, O₂, and CO*, *Journal of Applied Physics* **73**(12), 1993, pp. 8371–6.
- [23] KUPRIYANOW L.YU., *Semiconductor Sensors in Physico-Chemical Studies*, Elsevier, Amsterdam 1996.

*Received May 14, 2007
in revised form July 23, 2007*